ICARUS 33, 514–528 (1978)

Theoretical Models for Mars and Their Seismic Properties

EMILE A. OKAL AND DON L. ANDERSON

Seismological Laboratory, California Institute of Technology, Pasadena, California 91125

Received April 27, 1977; revised July 25, 1977

Theoretical seismic properties of the planet Mars are investigated on the basis of the various models which have been proposed for the internal composition of the planet. The latest interpretation of gravity field data (Reasenberg, 1977), assuming a lower value of the moment of inertia, would require a less dense mantle and a larger core than previous models. If Mars is chondritic in composition, the most reasonable models are an incompletely differentiated H-chondrite or a mixture of H-chondrites and carbonaceous chondrites. Seismic profiles, travel times, and free oscillation periods are computed for various models, with the aim of establishing which seismic data is crucial for deciding among the alternatives. A detailed discussion is given of the seismic properties which could—in principle—help answer the following two questions: Is Mars' core liquid or solid? Does Mars have a partially molten asthenosphere in its upper mantle?

INTRODUCTION

The purpose of this paper is to provide a number of seismic models of the planet Mars, derived theoretically from various recent models of the internal constitution of the planet, and to examine what kind of future seismic experiments could yield answers to crucial questions concerning the origin and state of Mars, namely, the physical state of its core and the possible existence of an asthenosphere involving partial melting.

The study of the internal structure of Mars can be traced back to Jeffreys (1937), who first proposed the existence of a dense core, on the basis of astronomical observations of the oblateness of the planet. Little further progress was made until 1965, when the Mariner 4 flyby mission provided close photographs of the surface. On the basis of this early data, a similarity to the Moon was inferred, leading to the idea of a possibly nondifferentiated planet, its core, if any, being very small (Binder, 1969).

In 1971, the Mariner 9 Orbiter experiment yielded a considerable amount of new data, including the value of the second harmonic of the gravity field:

$$J_2 = (1.96 \pm 0.01) \times 10^{-3}$$

(Lorell *et al.*, 1972). Assuming hydrostatic equilibrium, one could infer a value of the normalized moment of inertia about the polar axis

$$K = C/MR^2 = 0.377.$$

This value was used by Anderson (1972) to propose two models for the Martian interior, hereafter called A1 and A2:

Model A1 describes Mars as a mixture of 75% carbonaceous and 25% ordinary chondrites, totally differentiated.

Model A2 describes Mars as a partially differentiated ordinary chondrite, some Fe, Ni, and a little FeS remaining in the solid mantle. Johnston *et al.* (1974) computed two possible models for the thermal history of the planet, depending on an initially cool

0019-1035/78/0333-0514$02.00/0

(0°C) or hot (500°C) accretion. Their models (J1 and J2) differ by the presence of an olivine-spinel transition in the "hot" case (Model J2), which is absent from the cool one. Their models have smaller and denser cores than Anderson's. These authors also discuss the possible petrology of the mantle and the possibility of partial melting due to water in the upper mantle. Anderson (1973) also discussed the possibility of water in the interior of Mars. All four models (A1, A2, J1, J2) assume a liquid core. Although Ringwood (1977) has recently proposed that oxygen may be the light alloying element in the Earth's core, this requires temperatures larger than 1500°C which are improbable for Mars. This leaves sulfur a strong candidate as the light alloying element in Mars' core. A liquid core is then likely (Anderson, 1971). Although there remains a controversy on the existence of a Martian magnetic field (Dolginov *et al.*, 1972; Bogdanov and Vaisberg, 1975), an upper bound of 60γ has been proposed. According to Anderson (1972), this low magnitic field may be due to the small size and high resistivity of the Mars core, compared to the terrestrial core.

Another important discovery of the Mariner 9 mission was the evidence for tectonic activity on Mars (Masursky, 1973). Although no precise timetable of the evolution of the planet is available yet, evidence for tectonic and volcanic activity has been confirmed by the 1976 Viking missions. The nonhydrostatic shape of Mars suggests that high stresses may be maintained in the lithosphere. The previous interpretation of the gravitational field constant J_2 in terms of K is probably erroneous, and lower values of K, resulting from various models allowing for at least partial isostatic compensation of the crust have been proposed. Binder and Davis (1973) describe two models (hereafter B1 and B2) corresponding to $K = 0.376$ and $K = 0.372$. Both of these assume a solid core, which in their opinion is necessary to explain the absence of a substantial magnetic field. Model B1 allows for a spinel–postspinel transition in the deep mantle, which is absent from model B2. Reasenberg's (1977) model of a spheroid close to isostatic equilibrium with an extra mass in the Tharsis area, yields $K = 0.3654 \pm 0.001$ for the body which would result from the relaxation of the rigidity supporting Tharsis. This helps reconcile the optical and dynamical flattening data.

The question of the physical state (liquid vs solid) of the Martian core is still unresolved. Similarly, it is not known whether Martian volcanism orginates in an upper mantle zone of partial melting, as suggested by Johnston *et al.* (1974). Young and Schubert (1974) have shown that the answers to both questions might be related. One of the goals of the present paper is to examine which seismic experiments can potentially yield answers to these crucial questions. It will be assumed throughout the paper that seismic sources exist on the planet.

In the first section we show that Reasenberg's model ($K = 0.3654$) is still compatible with Anderson's (1972) two postulates concerning the composition of Mars, i.e., an incompletely differentiated ordinary (high iron) chondrite, or a mixture of ordinary and carbonaceous chondrites. In the second section, we use these models to calculate seismic velocity profiles, traveltime tables, and free oscillation periods. In the third section, we discuss the specific properties of these models, in relation to the physical state of the core, and the possibility of a zone of partial melting in the upper mantle of the planet.

1. THE POSSIBLE COMPOSITION OF MARS, RESULTING FROM REASENBERG'S MODEL

In this section, we use Anderson's (1972) approach to investigate how Reasenberg's value ($K = 0.3654$) constrains the possible composition of the planet. In Fig. 1,

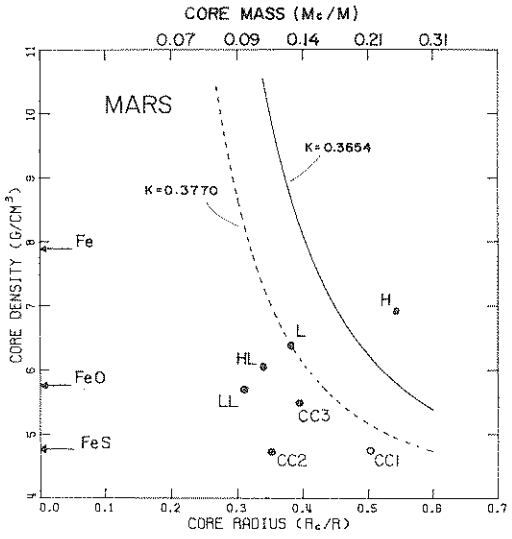

FIG. 1. Radius and mass of the core vs density of the core for Martian models with either $K = 0.377$ (dashed line) or $K = 0.3654$ (solid line). The dots represent various chondrites (see text and Table II) under the assumption of total differentiation [as in Anderson (1972, Fig. 1)].

adapted from Anderson (1972), we plot the density of the core, as a function of its radius for both values of K (0.377 in Anderson's model; 0.3654 in Reasenberg's). Similarly, Table I is adapted from Anderson's Table I. The assumption of a chondritic composition for Mars leads to values of the relative radius and mass of the core:

TABLE I

PARAMETERS FOR MARS MODELS, ASSUMING $K = C/MR^2 = 0.3654$

Core radius R_c/R	Mantle density ρ_m (g/cm³)	Core density ρ_c (g/cm³)	Core mass M_c/M
0.20	3.450	34.322	0.07
0.25	3.444	19.809	0.08
0.30	3.437	13.344	0.09
0.35	3.427	10.026	0.11
0.40	3.415	8.145	0.14
0.45	3.401	6.995	0.17
0.50	3.382	6.250	0.21
0.55	3.359	5.745	0.26
0.60	3.328	5.389	0.31

TABLE II

PARAMETERS FOR PURE CHONDRITE PLANETARY MODELS

Chondrite type	M_c/M	ρ_c (g/cm³)	ρ_m (g/cm³)
High iron, low metal (HL)	0.11	5.95	3.38
Low iron, low metal (LL)	0.10	5.83	3.38
Low iron hypersthene (L)	0.15	6.29	3.31
High iron (H)	0.24	6.95	3.26

$R_c/R = 0.50$ and $M_c/M = 0.21$. The core is therefore larger than in previous models. This results directly from the lower value of K. The density of the mantle is found to be lower than in previous models: $\rho_m \simeq 3.38$ g/cm³, which is less than the density of the silicate phase of most ordinary chondrites. Table II gives the fraction of core-forming material (Fe, Ni, FeS), the density of the siderophile fraction, and the density of the silicate fraction for several classes of ordinary chondrites. These figures are based on compositions given in Keil (1969), and on the assumption that all the sulfur reported as FeS is actually present in the potentially core-forming sulfide form.

HL (high iron, low metal) chondrites (ornasites), LL (low iron, low metal or amphetorites) and L (low iron or hypersthene-olivine) chondrites all have lower amounts of potentially core-forming material than is required for Mars in this model, although HL and LL have about the right silicate density (3.38 g/cm³). If completely differentiated, H (high iron) chondrites have too much core and also too small a silicate density (3.26–3.29 g/cm³). As in Anderson (1972), we can match the properties of H chondrites with Mars if we assume that the planet is incompletely differentiated. If the composition of the core-forming material is on the Fe side of the Fe–FeS eutectic, and temperatures in the mantle are above the eutectic composition, but below the liquidus, then the core will be more sulfur-rich and therefore less dense than the potential core-forming material, and the density of

the mantle larger than for the silicate fraction. In fact, if we reduce the Fe content of the potential core-forming material in H chondrites to the value required by Reasenberg's K, and place the remaining Fe in the mantle, the density of the mantle (silicate phase plus solid fraction of free iron) is 3.38 g/cm³.

A meteorite mixture is also possible: Anderson's model A1 can easily be adapted to fit Reasenberg's data. The resulting model (hereafter called AR) differs from A1 principally in its lower mantle density ($\rho_m = 3.38$ g/cm³) and larger core radius ($R_c/R = 0.50$). In the following section, we will derive a full seismic model for model AR, and will also mention results obtained for models J1 and J2 (Johnston *et al.*, 1974) and B1 and B2 (Binder and Davis, 1973), the latter two having a solid core.

2. CONSTRUCTING THE SEISMIC MODELS

The goal of this section is to investigate the differences between the various proposed models, particularly in their seismic response. The basis for the derivation of the seismic profiles from the assumed densities and compositions is Anderson's (1967) seismic equation of state,

$$\phi = \phi_0(\rho/\bar{M})^{1/E},$$

where $\phi = V_P^2 - \frac{4}{3}V_S^2 = k_s/\rho$ is the seismic parameter, ρ is the density, $\bar{M}$ is the mean atomic mass of the chemicals in the assumed phase, and ϕ_0 and E are constants, depending only on the type of material involved (silicate, liquid Fe-rich metal, or solid Fe-rich metal). V_P and V_S are the seismic compressional and shear velocities, and k_s is the modulus of incompressibility. Following Birch (1952), we will assume that ϕ is a function only of ρ, regardless of the nature of the effect which causes ρ to vary (pressure, temperature, phase change). The parameters ϕ_0 and E depend only on the type of material involved, and can be taken from various Earth models: In the case of the core, assumed liquid except in Binder and Davis' (1973) models B1 and B2, the values of ϕ_0 and E were computed from Anderson and Hart's (1976) seismic profile in the outer core of the Earth. In the case of the solid core of models B1 and B2, the values were taken from the inner-core part of the above model. In the case of the mantle, the theoretical models of Anderson (1967) were used, in order to avoid possible variations in the equation of state due to partial melting in the low velocity zone of the Earth. Values of $\bar{M}$ were computed from the various chemical compositions involved. Finally, values of the Poisson ratio, σ, were assigned as follows: Inside the mantle silicates, a value of 0.28 was taken, by analogy with the values derived from the Earth model C2 (Anderson and Hart, 1976). Inside the solid core of models B1 and B2, a value of 0.30 was adopted, corresponding to pure iron under normal conditions: it seemed unwarranted to take the very high value ($\sigma = 0.444$) associated with the Earth's inner core, since the extreme pressure and temperature conditions responsible for it are not appropriate for the interior of Mars. Table III summarizes all the numerical data used in the computation of the various models.

Figure 2 and Table IV show the resulting seismic profile for model AR; Fig. 2 also shows seismic profiles for models J1, J2, B1, and B2. Three major features are apparent on this figure:

(*i*) *The velocities are usually lower than in the Earth.* This is due mainly to Mars' lower density, itself due to lower gravity. The only exception is Binder and Davis' model B1 which has a relatively smaller core, with a dense, highly compressed, and consequently fast, postspinel phase in the lower mantle.

(*ii*) *The velocities are relatively constant* within a given mineralogical phase. This is

TABLE III

SUMMARY OF PARAMETERS USED IN THE COMPUTATION OF THE VARIOUS SEISMIC MODELS

Model	Phase	Radius range (km)	$\bar{M}$ (g)	ρ_m (g/cm^3)	E	ϕ_0[a]	σ	K
AR	Core	0–1694	50.2	3.38	0.381	4 519	0.5	0.3654
	Spinel	1694–2255	22.1		0.323	12 102	0.28	
	Olivine	2255–3338	22.1		0.323	12 102	0.28	
	[Crust]	3338–3388						
J1	Core	0–1338	50.25	3.69	0.381	4 519	0.5	0.377
	Mantle	1338–3338	23.79		0.323	12 102	0.28	
	[Crust]	3338–3388						
J2	Core	0–1238	50.25	3.65	0.381	4 519	0.5	0.377
	Spinel	1238–2164	23.79		0.323	12 102	0.28	
	Olivine	2164–3338	23.79		0.323	12 102	0.28	
	[Crust]	3338–3388						
B1	Core	0–1031	53.97	3.52	0.3935	3 882	0.30	0.376
	Postspinel	1031–1553	22.54		0.323	12 102	0.28	
	Spinel	1553–2275	22.54		0.323	12 102	0.28	
	Olivine	2275–3328	22.54		0.323	12 102	0.28	
	[Crust]	3328–3388						
B2	Core	0–1359	49.97	3.52	0.3935	3 882	0.30	0.372
	Spinel	1359–2410	22.16		0.323	12 102	0.28	
	Olivine	2410–3328	22.16		0.323	12 102	0.28	
	[Crust]	3328–3388						

[a] Units for ϕ_0 are such that ϕ is in (km/sec)^2, $\bar{M}$ in g, and ρ in g/cm^3.

due to the lower compression in Mars' interior, resulting from the lower density and lower gravity. Consequently, the seismic rays inside a given chemical phase are expected to be substantially less refracted than in the Earth.

(*iii*) *The discontinuity at the core–mantle boundary (CMB) is large.* The velocity drops from values ranging from 10 to 13 km/sec to values of 4.7 km/sec in the case of a liquid core and 6–7 km/sec in the case of models B1 and B2. This is again due to the small size of the planet, which implies less pressure in the core. Refraction at the CMB is therefore expected to be drastic.

For each of the models studied, it is then possible to obtain travel-time tables for various seismic phases, and to compute an estimate of the free oscillation periods of the planet.

A. Travel times for surface focus *P*, *PKP*, *PcP*, *S*, *SKS*, *ScS* in model AR are listed in Tables Va–e. No attempt was made to tabulate *P* and *S* at the shorter distances ($\Delta < 20°$): these seismic phases would be very dependent upon the nature of the Martian crust and upper mantle, which is still poorly known. Figure 3 shows a set of travel-time curves.

a. Mantle waves (P, S). Apart from the low curvature of the travel-time curves, due to the planet's low compression, the main feature of this model is the triplication due to the olivine–spinel transition. Such a feature is absent from the "cool" model J1 of Johnston *et al.* (1974), and two such triplications are observed for Binder and

Davis' (1973) model B1, which has a postspinel phase in the lower mantle. The range of distances at which this transition is observed is characteristic of the various models: It varies from 45° in model AR to 61° in model J2. Thus, besides resolving the absence or presence of the transition, the study of the triplication could prove very useful in the investigation of the planet: due to Mars' low density, a small variation in the temperature field moves the transition up or down in the mantle substantially, thereby displacing the triplication considerably along the surface.

b. PcP and ScS, phases reflected from the core, could provide a strong constraint on the core's radius and physical state. Both models B1 and B2 give very low (~10%) reflection coefficients for vertical *ScS*, which implies that these phases should not be observed if the core is solid.

c. The core phases PKP and SKS are, for diagnostic purposes, the most promising phases in Martian seismology. As a result of the general features listed earlier, *P* waves reaching the core are very sharply refracted into the core, and then continue along nearly straight ray paths across the core. At their emergence, they are again sharply refracted, the result being that nearly every ray going through the core, in every model, emerges at a distance larger than 180°. Figure 4 illustrates this situation and compares it with the Earth, as described by Julian and Anderson (1968). The resulting shadow zone is apparent on Fig. 3, in which the *PKP* branch has been folded about the 180° axis. This

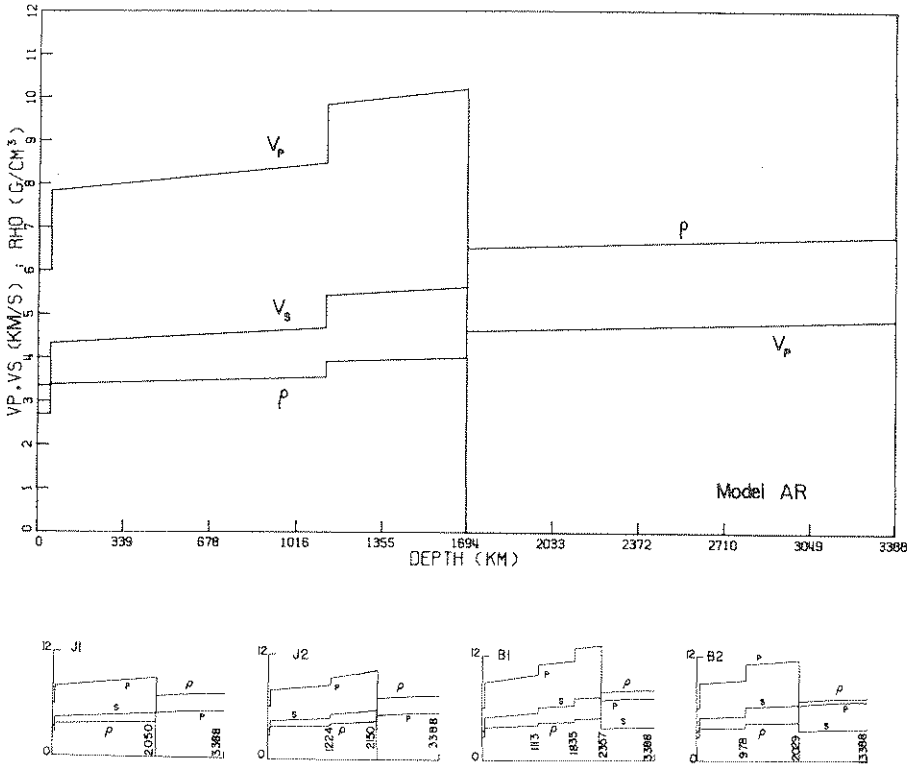

FIG. 2. Density and seismic velocity profiles for model AR, as obtained in this study. The four small diagrams schematically describe similar profiles for models J1, J2, B1, and B2. The scale (0 to 12) is the same for all of them. The depths of the various discontinuities listed in Table III are shown for each model.

TABLE IV

SEISMIC VELOCITIES AND DENSITIES IN MODEL AR

Radius (km)	Depth (km)	V_P (km/sec)	V_S (km/sec)	ρ (g/cm³)	Radius (km)	Depth (km)	V_P (km/sec)	V_S (km/sec)	ρ (g/cm³)
0	3388	4.891	0.0	6.815	1750	1638	10.169	5.621	4.008
50	3338	4.883	0.0	6.807	1800	1588	10.136	5.603	4.000
100	3288	4.875	0.0	6.798	1850	1538	10.103	5.585	3.991
150	3238	4.867	0.0	6.790	1900	1488	10.071	5.567	3.983
200	3188	4.859	0.0	6.782	1950	1438	10.038	5.549	3.975
250	3138	4.851	0.0	6.773	2000	1388	10.006	5.531	3.966
300	3088	4.844	0.0	6.765	2050	1338	9.973	5.513	3.958
350	3038	4.836	0.0	6.757	2100	1288	9.941	5.495	3.950
400	2988	4.828	0.0	6.748	2150	1238	9.908	5.477	3.941
450	2938	4.820	0.0	6.740	2200	1188	9.876	5.459	3.933
500	2888	4.812	0.0	6.732	2250	1138	9.843	5.441	3.925
550	2838	4.805	0.0	6.723	2255	1133	9.840	5.439	3.924
600	2788	4.797	0.0	6.715	2255	1133	8.493	4.695	3.568
650	2738	4.789	0.0	6.707	2300	1088	8.465	4.679	3.560
700	2688	4.781	0.0	6.698	2350	1038	8.435	4.663	3.552
750	2638	4.773	0.0	6.690	2400	988	8.404	4.646	3.544
800	2588	4.765	0.0	6.682	2450	938	8.374	4.629	3.535
850	2538	4.758	0.0	6.673	2500	888	8.343	4.612	3.527
900	2488	4.750	0.0	6.665	2550	838	8.313	4.595	3.519
950	2438	4.742	0.0	6.657	2600	788	8.282	4.578	3.510
1000	2388	4.734	0.0	6.648	2650	738	8.252	4.561	3.502
1050	2338	4.726	0.0	6.640	2700	688	8.221	4.544	3.494
1100	2288	4.719	0.0	6.632	2750	638	8.191	4.528	3.485
1150	2238	4.711	0.0	6.623	2800	588	8.161	4.511	3.477
1200	2188	4.703	0.0	6.615	2850	538	8.130	4.494	3.469
1250	2138	4.695	0.0	6.607	2900	488	8.100	4.477	3.460
1300	2088	4.688	0.0	6.598	2950	438	8.070	4.461	3.452
1350	2038	4.680	0.0	6.590	3000	388	8.040	4.444	3.444
1400	1988	4.672	0.0	6.582	3050	338	8.010	4.427	3.435
1450	1938	4.664	0.0	6.573	3100	288	7.980	4.411	3.427
1500	1888	4.656	0.0	6.565	3150	238	7.949	4.394	3.419
1550	1838	4.649	0.0	6.557	3200	188	7.919	4.378	3.410
1600	1788	4.641	0.0	6.548	3250	138	7.890	4.361	3.402
1650	1738	4.633	0.0	6.540	3300	88	7.860	4.345	3.394
1694	1694	4.626	0.0	6.532	3338	50	7.843	4.335	3.389
1694	1694	10.206	5.641	4.017	3338	50	6.000	3.360	2.700
1700	1688	10.202	5.639	4.016	3388	0	6.000	3.360	2.700

branch is extremely sensitive to variations in the seismic model. As expected, the size of the core plays a dominant role: the rays are more sharply bent around a smaller core. Anderson's (1972) original model A1 exhibits a *PKP* branch extending all the way back to 241° (or 119°), thereby considerably reducing the shadow zone. Also, in a recent study, Johnston and Toksöz (1977) have proposed a range of seismic models of Mars, based on theoretical calculations of the thermal evolution of the planet. In general, their results ask for velocities slower than in model AR, especially in the deep mantle. This model does not allow for *PKP* phases at $\Delta > 180°$. This difference arises from the fact that Johnston and Toksöz's model allows only

for a small density increase at the olivine–spinel transition (3.2% in density or 5.3% in V_P); as a result, their velocities at the base of the mantle are only on the order of 8.8 km/sec (as compared with 10.2 km/sec in model AR) and the velocity contrast at the CMB is not sufficient to bend the *PKP* rays past 180°. However, the model of these authors predicts a shadow zone from 90 to 150°.

The possibility of actually observing *PKP* on Mars from a moderately sized event seems fair, despite the large geometrical spreading at the CMB. The theoretical relative amplitudes (Bullen, 1953),

$$A = [\tan i \,|di/d\Delta|\,(1/|\sin \Delta|)]^{1/2}$$

(i being the angle of incidence of the ray at the Earth's surface), are found to be 0.272 for *P* at 100° and 0.167 for *PKP* at 209° in model AR, a ratio smaller than 2. Thus according to Anderson *et al.* (1976), an event with $m_b = 6.3$ at 210° (150°) should yield observable *PKP*'s, for a detection threshold of 3×10^{-9} m surface displacement (Anderson *et al.*, 1977). Note that on Fig. 4, the incidence sampling is increased from 1 to 0.1° near critical incidence at the CMB. However, these figures could be altered by the attenuation factor Q, a quantity totally unknown for Mars and the Martian core at the present time.

On Fig. 3, *SKS* appears not to be linked continuously to *S*, as is the case in the Earth. This is due to a drop in velocity between lower mantle *S* waves ($\beta = 5.64$ km/sec) and *K* waves ($\alpha = 4.62$ km/sec) at the CMB. This results in a shadow zone for *S*, extending from 104 to 145° in model AR. (The fact that the upper limit of the *S* shadow zone roughly coincides with that of the *PKP* one is a pure artifact of the folding of the *PKP* branch about the 180° axis.) This *S* shadow zone is very small in model B2, and is absent from the "cool," homogeneous mantle, model J1. However,

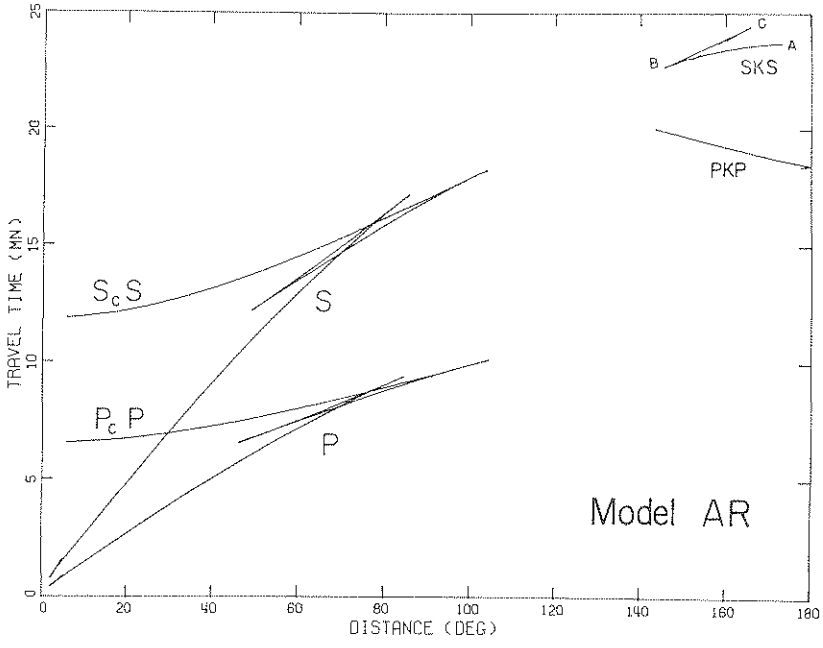

FIG. 3. Travel-time curves for *P*, *PcP*, *PKP*, *S*, *ScS*, *SKS* in model AR. Note that *PKP* has been folded about the 180° axis.

TABLE Va

SURFACE FOCUS P TIMES FOR MODEL AR

Δ (deg)	P (sec)	Δ (deg)	P (sec)	Δ (deg)	P (sec)
20	158.6	49	359.9	77	512.8
21	165.9	50	366.4	78	516.5
22	173.2	51	372.8	79	520.2
23	180.4	52	379.2	80	523.9
24	187.6	53	385.5	81	527.6
25	194.8	54	391.8	82	531.2
26	202.0	55	398.1	83	534.8
27	209.2	56	404.3	84	538.4
28	216.3	57	410.5	85	541.9
29	223.5	58	416.6	86	545.5
30	230.6	59	422.7	87	549.0
31	237.7	60	428.8	88	552.5
32	244.7	61	434.8	89	555.9
33	251.7	62	440.7	90	559.3
34	258.7	63	446.6	91	562.7
35	265.7	64	452.5	92	566.0
36	272.6	65	458.3	93	569.4
37	279.5	66	464.1	94	572.7
38	286.4	67	469.8	95	575.9
39	293.3	68	475.5	96	579.2
40	300.1	69	481.1	97	582.3
41	306.9	70	486.3	98	585.5
42	313.6	71	490.1	99	588.6
43	320.3	72	493.9	100	591.7
44	327.0	73	497.7	101	594.8
45	333.7	74	501.5	102	597.8
46	340.3	75	505.3	103	600.7
47	346.9	76	509.0	104	603.7
48	353.4				

a major difference between J1 and B2 remains the very low amplitudes of transversely polarized *ScS* in model B2.

B. Free oscillation periods were computed for the various models involved. Tables VIa, b list the values of the periods of the torsional modes ${}_0T_l$ ($l \leq 10$). As expected, the size and state of the core are the main factor governing the eigenperiods for low values of l. A solid core sharply decreases the eigenperiods, as does, to a lesser extent, an increase in the size of a liquid core. Overtones ${}_nT_l$ would undergo a totally different behavior, depending on whether the core is solid or liquid (Okal, 1977). However, these are most unlikely to be observed and also, this property is the normal-mode counterpart of the different behavior of *ScS*, in ray theory. Therefore the overtones were not computed. It should be pointed out that, due to the relative homogeneity of the mantle, the modes have a rather constant phase velocity, itself resulting in a smooth group velocity. Table VIb shows that the phase velocity varies only from 4.92 km/sec at 412 sec to 5.12 km/sec at 757 sec for model AR (a 4% difference), as opposed to the corresponding figures for the Earth (6.40 km/sec at 739 sec and 5.59 km/sec at 409 sec, a 15% difference). This property of relatively constant phase velocities along the fundamental branch might help identify normal modes by using a sequence of them to assign angular orders: A family of modes should closely obey a relation of the form $(l + \frac{1}{2})/\omega_l = cst$. This makes it possible to discriminate between models with otherwise similar periods (e.g., ${}_0T_9$ for model B2 and ${}_0T_{10}$ for J1 have about the same period: 405 sec).

TABLE Vb

SURFACE FOCUS *PKP* TIMES FOR MODEL AR

Δ (deg)	*PKP* (sec)	Δ (deg)	*PKP* (sec)
178	1106.0	198	1153.0
179	1107.5	199	1155.8
180	1109.3	200	1158.6
181	1111.2	201	1161.3
182	1113.3	202	1164.1
183	1115.4	203	1166.9
184	1117.6	204	1169.7
185	1119.9	205	1172.5
186	1122.2	206	1175.3
187	1124.6	207	1178.1
188	1127.1	208	1180.9
189	1129.6	209	1183.7
190	1132.1	210	1186.6
191	1134.6	211	1189.4
192	1137.1	212	1192.3
193	1139.7	213	1195.1
194	1142.3	214	1198.0
195	1144.9	215	1200.8
196	1147.6	216	1203.7
197	1150.3		

Tables VIIa, b similarly list periods and surface-wave phase and group velocities for the spheroidal oscillations of the planet. Models with a solid core (B1, B2) have fundamental periods for ${}_0S_2$ on the order of 1300–1400 sec, much shorter than the corresponding periods for models with a liquid core (1800–2400 sec). The period of ${}_0S_2$ is a very powerful constraint on the Martian interior. Its observation would, however, depend on the installation of long-period instruments.

3. TWO QUESTIONS WHICH SEISMOLOGY MIGHT ANSWER

A. Is Mars' core liquid or solid? The existence of a Martian core has been proved during the Mariner 9 mission: The value of J_2 and the upper bound on that of $K = C/MR^2$ are incompatible with the hypothesis of an undifferentiated planet. It would be extremely important to solve the question of the state of the core of Mars: If Mars has a liquid core, then it had a hot thermal history and the models of Anderson (1972) and Johnston *et al.* (1974) show that the core has to include an alloying element—presumably sulfur—to account for its low density. The decrease in core resistivity could in turn be responsible for the planet's low magnetic field. This would put new constraints on possible mechanisms driving the Earth's dynamo. If, on the other hand, Mars has a solid core, its

TABLE Vc

SURFACE FOCUS *S* TIMES FOR MODEL AR

Δ (deg)	*S* (sec)	Δ (deg)	*S* (sec)	Δ (deg)	*S* (sec)
20	286.4	49	650.6	77	927.4
21	299.5	50	662.3	78	934.1
22	312.7	51	673.9	79	940.8
23	325.8	52	685.5	80	947.4
24	338.9	53	697.0	81	954.0
25	351.9	54	708.4	82	960.5
26	364.9	55	719.7	83	967.1
27	377.9	56	731.0	84	973.5
28	390.8	57	742.1	85	980.0
29	403.7	58	753.2	86	986.4
30	416.6	59	764.3	87	992.7
31	429.4	60	775.2	88	999.0
32	442.1	61	786.0	89	1005.2
33	454.8	62	796.8	90	1011.4
34	467.5	63	807.5	91	1017.5
35	480.1	64	818.1	92	1023.6
36	492.6	65	828.6	93	1029.6
37	505.2	66	839.1	94	1035.6
38	517.6	67	849.4	95	1041.4
39	530.0	68	859.7	96	1047.3
40	542.3	69	869.9	97	1053.0
41	554.6	70	879.1	98	1058.7
42	566.8	71	886.1	99	1064.4
43	579.0	72	893.1	100	1070.0
44	591.1	73	900.1	101	1075.5
45	603.1	74	906.9	102	1080.9
46	615.1	75	913.8	103	1086.3
47	627.0	76	920.6	104	1091.7
48	638.8				

TABLE Vd

SURFACE FOCUS *SKS* TRAVEL TIMES FOR MODEL AR

Δ (deg)	SKS_{AB} (sec)	SKS_{BC} (sec)
146	1364.8	1365.0
147	1368.7	1369.8
148	1372.4	1374.6
149	1376.0	1379.5
150	1379.4	1384.5
151	1382.6	1389.6
152	1385.6	1394.6
153	1388.6	1399.8
154	1391.5	1404.9
155	1394.2	1410.0
156	1396.7	1415.2
157	1399.2	1420.3
158	1401.5	1425.4
159	1403.6	1430.6
160	1405.7	1435.8
161	1407.6	1441.0
162	1409.5	1446.2
163	1411.2	1451.4
164	1412.9	1456.6
165	1414.4	1461.9
166	1415.8	
167	1417.1	
168	1418.3	
169	1419.3	
170	1420.3	
171	1421.2	
172	1422.0	
173	1422.6	

TABLE Ve

SURFACE FOCUS *PcP* AND *ScS* TRAVEL TIMES FOR MODEL AR

Δ (deg)	*PcP* (sec)	*ScS* (sec)	Δ (deg)	*PcP* (sec)	*ScS* (sec)	Δ (deg)	*PcP* (sec)	*ScS* (sec)
0	394.1	712.6	34	425.1	768.7	67	499.4	903.1
1	394.1	712.6	35	426.9	771.9	68	502.1	907.9
2	394.2	712.8	36	428.7	775.1	69	504.8	912.8
3	394.4	713.0	37	430.5	778.4	70	507.4	917.6
4	394.6	713.4	38	432.4	781.8	71	510.1	922.5
5	394.8	713.8	39	434.3	785.2	72	512.9	927.4
6	395.1	714.4	40	436.2	788.7	73	515.6	932.3
7	395.5	715.1	41	438.2	792.3	74	518.3	937.3
8	395.9	715.8	42	440.2	795.9	75	521.0	942.2
9	396.4	716.7	43	442.2	799.6	76	523.8	947.2
10	396.9	717.6	44	444.3	803.4	77	526.5	952.2
11	397.5	718.7	45	446.4	807.2	78	529.3	957.2
12	398.2	719.9	46	448.6	811.1	79	532.1	962.2
13	398.9	721.1	47	450.7	815.0	80	534.9	967.3
14	399.6	722.5	48	452.9	819.0	81	537.7	972.4
15	400.4	724.0	49	455.2	823.1	82	540.5	977.5
16	401.3	725.5	50	457.4	827.2	83	543.4	982.6
17	402.2	727.2	51	459.7	831.3	84	546.2	987.7
18	403.1	728.9	52	462.0	835.5	85	549.0	992.8
19	404.2	730.7	53	464.4	839.7	86	551.9	997.9
20	405.2	732.7	54	466.7	844.0	87	554.7	1003.1
21	406.3	734.7	55	469.1	848.3	88	557.6	1008.3
22	407.5	736.8	56	471.6	852.6	89	560.4	1013.4
23	408.7	739.0	57	474.0	857.0	90	563.3	1018.6
24	410.0	741.3	58	476.5	861.5	91	566.1	1023.8
25	411.3	743.7	59	479.0	866.0	92	569.0	1029.0
26	412.7	746.1	60	481.4	870.5	93	571.9	1034.2
27	414.1	748.7	61	484.0	875.1	94	574.8	1039.4
28	415.5	751.3	62	486.5	879.7	95	577.6	1044.6
29	417.0	754.0	63	489.1	884.3	96	580.5	1049.8
30	418.6	756.8	64	491.6	889.0	97	583.4	1055.1
31	420.1	759.7	65	494.2	893.6	98	586.3	1060.3
32	421.8	762.6	66	496.8	898.4	99	589.2	1065.5
33	423.4	765.6						

thermal regime must be cool. Young and Schubert (1974) have proposed that this might be the result of large-scale convection in the mantle. Martian volcanism would then presumably be ancient. From the former section, it is clear that, for all plausible models, the following seismic observations would resolve the nature of the Martian core:

In favor of a liquid core:

Strong $(ScS)_{SH}$ waves at near vertical incidence,

A shadow zone for *SKS* at 100–140°,

A fundamental ($_0S_2$) period of 1800–2400 sec.

In favor of a solid core:

Weak $(ScS)_{SH}$ waves at near vertical incidence,

An *SKS* phase between 100 and 140°,

A fundamental ($_0S_2$) period of 1200–1500 sec.

B. Does Mars have an asthenosphere? The interpretation of photographic and

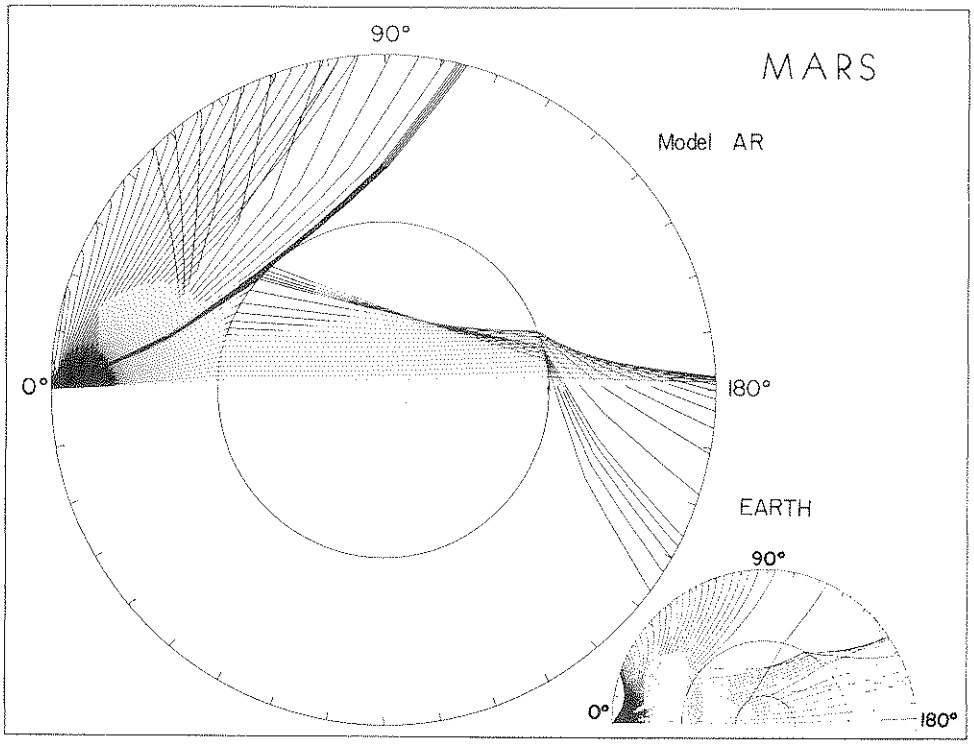

FIG. 4. Ray paths for P and PKP inside Mars for model AR. A surface-focus event is assumed. The take-off angle varies from 1 to 50° in 1° increments, and from 16.5 to 17.5° in 0.1° increments. The smaller diagram [reproduced from Julian and Anderson (1968, Fig. 9)], compares with the Earth.

gravity data has led to a picture of a very rugged Martian surface. Hawaiian-type volcanism has been inferred from surface topography with altitudes as high as 23 km (Wu *et al.*, 1973). It has been proposed that this volcanism is associated with a low-viscosity flow of lavas (Carr, 1973), and it is reasonable to think of the possibility of a zone of partial melting (ZPM) in the upper mantle. On the other hand, no apparent present plate tectonic activity has been reported (Masursky 1973) and the age of the Martian volcanoes is still unknown.

A ZPM should cause a seismic low-velocity zone (LVZ), in a way similar to the Earth's LVZ. Johnston *et al.* (1974) studied the phase diagrams of eclogite (their candidate for the Martian mantle) in the presence of 0.1 to 0.2% water. Water is present in the atmosphere, the residual polar caps, and was formerly present on the surface. Such a small amount of water would be low enough not to affect the mass and moment of inertia calculations, but would cause eclogite to undergo partial melting at a depth on the order of 200 km. Because of the height of the relief on the Martian surface, it is thought that the lithosphere could, by isostasy, reach such a depth. This figure is also consistent with the apparent lack of plate tectonic activity (Masursky, 1973), with a tentative estimate of the depth of the magma chamber of Nix Olimpica (Carr, 1973), and with the large distances between Martian volcanoes (Lingenfelter and Schubert, 1974).

It is therefore of interest to test seismic models including an LVZ. The starting model for these computations was Ander-

TABLE VIa

PERIODS OF TORSIONAL OSCILLATIONS (sec) FOR A NUMBER OF MODELS

Mode	AR	J1	J2	B1	B2
${}_0T_2$	1865	1865	1843	1563	1597
${}_0T_3$	1209	1207	1208	1039	1055
${}_0T_4$	924	919	927	802	815
${}_0T_5$	757	750	760	680	673
${}_0T_6$	645	638	647	564	576
${}_0T_7$	564	556	565	494	506
${}_0T_8$	502	494	502	440	450
${}_0T_9$	452	445	453	397	406
${}_0T_{10}$	412	405	412	362	371

TABLE VIb

LOVE-WAVE PHASE AND GROUP VELOCITIES IN MODEL AR

Mode	Period (sec)	Phase velocity (km/sec)	Group velocity (km/sec)
${}_0T_2$	1865	4.57	6.19
${}_0T_3$	1209	5.03	5.43
${}_0T_4$	924	5.12	5.08
${}_0T_5$	757	5.11	4.88
${}_0T_6$	645	5.08	4.74
${}_0T_7$	564	5.03	4.66
${}_0T_8$	502	4.99	4.69
${}_0T_9$	452	4.96	4.57
${}_0T_{10}$	412	4.92	

son's (1972) original model A1. In order to ease certain computations carried out from the center of the planet, we assumed a depth of 188 km to the top of the LVZ. The drop of velocity at that depth was taken as equal in percentage (7%) to that observed in the Earth (Helmberger, 1973). It is more difficult to decide on the bottom depth of the LVZ: In the Earth, accumulated pressure is responsible for a relatively narrow LVZ. In the case of Mars, the effect of pressure with depth is slow; furthermore the geotherms are still tentative, and they seem to parallel the wet solidus, according to the phase diagram calculations of Johnston *et al.* Three models were tested, with LVZ's respectively 50, 200, and 350 km thick, these high values being due to low-pressure gradients. As expected, a strong body-wave shadow zone is developed, whereas the rest of the travel-time curves is mostly unaffected. However, no substantial difference is found between the three models in terms of the size of the shadow zone itself, which ranges from 9 to 21° in all cases. In the case of a small (2%) velocity decrease in the LVZ, as proposed by Johnston and Toksöz (1977), the shadow zone would merely be replaced by a zone of lower amplitudes. Free oscillation periods are slightly increased by the presence of the LVZ, especially for the 350-km thickness (on the order of 10 sec, or 2.5% at 400 sec). The eigenperiods would

TABLE VIIa

PERIODS OF SPHEROIDAL OSCILLATIONS (sec) FOR A NUMBER OF MODELS

Mode	AR	J1	J2	B1	B2
${}_0S_2$	2358	2083	1869	1284	1418
${}_0S_3$	1455	1277	1156	873	928
${}_0S_4$	1030	932	872	712	728
${}_0S_5$	797	752	728	612	617
${}_0S_6$	658	643	636	541	545
${}_0S_7$	571	567	568	486	491
${}_0S_8$	511	509	513	441	448
${}_0S_9$	465	463	469	404	410
${}_0S_{10}$	428	425	431	376	385

TABLE VIIb

RAYLEIGH-WAVE PHASE AND GROUP VELOCITIES IN MODEL AR

Mode	Period (sec)	Phase velocity (km/sec)	Group velocity (km/sec)
${}_0S_2$	2358	3.61	5.60
${}_0S_3$	1455	4.18	6.04
${}_0S_4$	1030	4.59	6.04
${}_0S_5$	797	4.86	5.64
${}_0S_6$	658	4.98	4.93
${}_0S_7$	571	4.97	4.38
${}_0S_8$	511	4.90	4.12
${}_0S_9$	465	4.82	3.96
${}_0S_{10}$	428	4.74	

not be sufficiently affected to change any conclusion reached about the solidity of the core.

The observation of a shadow zone (or of a zone of lower amplitudes) in P and S waves between 9 and 21° (530 and 1240 km) would prove the existence of a ZPM under the Martian lithosphere. Together with the physical state of the core, the answer to this question would be a great leap in our knowledge of Mars, and, retrospectively, of the Earth.

CONCLUSIONS

Models for the interior of Mars have been constructed on the basis of the revised moment of inertia (Reasenberg, 1977). The core is larger and denser than in previous models, and the mantle is less dense. A partially differentiated H-chondrite or a meteorite mixture model can still satisfy the constraints.

A set of theoretical values for travel times and free oscillation periods has been obtained for various models of the planet's interior. These seismological results can be used as a reference framework for future seismic exploration of the planet. Although these model are still tentative, they exhibit major differences which result from different assumptions for the Martian interior. Essential questions concerning Mars' core (is it solid or liquid?) and upper mantle (is there partial melting under the lithosphere?) could be answered by seismology, especially through the use of long-period instrumentation.

ACKNOWLEDGMENTS

Discussion over an early draft of this paper with Bob Geller, Seth Stein, and Bernard Minster is gratefully acknowledged. I thank Steve Smith for comments on some geochemical problems. Dave Johnston, Nafi Toksöz, and Ted Ringwood kindly made preprints available. Some of the computer programs used in this work were initially written by Bruce Julian and by Hiroo Kanamori. This research was supported by NASA, Contract NGL-05-002-069. Contribution Number 2902, Division of Geological and Planetary Sciences, California Institute of Technology.

REFERENCES

Anderson, D. L. (1967). A seismic equation of state. *Geophys. J. Roy. Astron. Soc.* **13**, 9–30.

Anderson, D. L. (1971). Sulfur in the core: Implications for the Earth and Mars. *Comments Earth Sci.* **1**, 133–137.

Anderson, D. L. (1972). Internal constitution of Mars. *J. Geophys. Res.* **77**, 789–795.

Anderson, D. L. (1973). The Moon as a high temperature condensate. *Moon* **8**, 33–57.

Anderson, D. L., and Hart R. S. (1976). An Earth model based on free oscillations and body waves. *J. Geophys. Res.* **81**, 1461–1475.

Anderson, D. L., Duennebier, F. K., Latham, G. V., Toksöz, M. N., Kovach, R. L., Knight, T. C. D., Lazarewicz, A. R., Miller, W. F., Nakamura, Y., and Sutton, G. (1976). The Viking seismic experiment. *Science* **194**, 1318–1321.

Anderson, D. L., Miller, W. F., Latham, G. V., Nakamura, Y., Toksöz, M. N., Dainty, A. M., Duennebier, F. K., Lazarewicz, A. R., Kovach, R. L., and Knight, T. C. D. (1977). Seismology on Mars. *J. Geophys. Res.* **82**, 4524–4546.

Binder, A. P. (1969). Internal structure of Mars. *J. Geophys. Res.* **74**, 3110–3118.

Binder, A. P., and Davis, D. R. (1973). Internal structure of Mars. *Phys. Earth Planet. Interiors* **7**, 477–485.

Birch, F. (1952). Elasticity and constitution of the Earth's interior. *J. Geophys. Res.* **57**, 227–286.

Bogdanov, A. V., and Vaisberg, O. L. (1975). Structure and variations of solar wind–Mars interaction region. *J. Geophys. Res.* **80**, 487–494.

Bullen, K. E. (1953). *An Introduction to the Theory of Seismology.* Cambridge Univ. Press, London/New York.

Carr, M. H. (1973). Volcanism on Mars. *J. Geophys. Res.* **78**, 4049–4062.

Dolginov, Sh. Sh., Eroshenko, E. G., and Zhuzgov, L. N. (1972). The magnetic field of Mars, according to data from the Mars 2 and Mars 3 spacecraft. *Dokl. Akad. Nauk SSSR* **207**, 1296–1299 (In Russian).

Helmberger, D. V. (1973). On the structure of the low-velocity zone. *Geophys. J. Roy. Astron. Soc.* **34**, 251–263.

Jeffreys, H. (1937). The density distribution of the inner planets. *Mon. Not. Roy. Astron. Soc., Geophys. Suppl.* **4**, 62–71.

Johnston, D. H., McGetchin, T. R., and Toksöz, M. N. (1974). The thermal state and internal structure of Mars. *J. Geophys. Res.* **79**, 3959–3971.

JOHNSTON, D. H., AND TOKSÖZ, M. N. (1977). Internal structure and properties of Mars. *Icarus* **32**, 73–84.

JULIAN, B. R., AND ANDERSON, D. L. (1968). Travel-times, apparent velocities and amplitude of body waves. *Bull. Seismol. Soc. Amer.* **58**, 339–366.

KEIL, K. (1969). Meteorite composition. In *Handbook of Geochemistry* (K. H. Wedepohl, Ed.), Vol. 1, pp. 78–115. Springer Verlag, Berlin/New York.

LINGENFELTER, R. E., AND SCHUBERT, G. (1974). Hotspot and trench volcano separation. *Nature* **249**, 820–821.

LORELL, J., BORN, G. H., CHRISTENSEN, E. J., JORDAN, J. F., LAING, P. A., MARTIN, W. L., SJOGREN, W. L., SHAPIRO, I. I., REASENBERG, R. D., AND SLATER, G. L. (1972). Mariner 9 celestial mechanics experiment: Gravity field and pole direction of Mars. *Science* **175**, 317–320.

MASURSKY, H. (1973). An overview of geological results from Mariner 9. *J. Geophys. Res.* **78**, 4009–4030.

OKAL, E. A. (1977). A physical classification of the Earth's spheroidal modes. *J. Phys. Earth*, in press.

PHILIPS, R. J., SAUDERS, R. S., AND CONEL, J. E. (1973). Mars: Crustal structure inferred from Bouguer anomalies. *J. Geophys. Res.* **78**, 4815–4820.

REASENBERG, R. D. (1977). The moment of inertia and isostasy of Mars. *J. Geophys. Res.* **82**, 369–375.

RINGWOOD, A. E. (1977). Composition of the core and implications for the origin of the Earth. Preprint.

WOOD, J. A. (1963). Physics and Chemistry of Meteorites. In *The Moon, Meteorites, and Comets* (B. M. Middlehurst and G. P. Kuiper, Eds.), pp. 337–401. Univ. of Chicago Press, Chicago.

WU, S. S. C., SCHAFER, F. J., NAKATA, G. M., JORDAN, R., AND BLASIUS, K. R. (1973). Photogrammetric evaluation of Mariner 9 photography. *J. Geophys. Res.* **78**, 4405–4410.

YOUNG, R. E., AND SCHUBERT, G. (1974). Temperatures inside Mars: Is the core liquid or solid? *Geophys. Res. Lett.* **1**, 157–160.